Electronic Supplementary Material (ESI) for Journal of Materials Chemistry A.

Supplementary Material

Synergizing internal electric field and ferroelectric polarization of $BiFeO_3/ZnIn_2S_4$ Z-scheme heterojunction for photocatalytic overall water splitting

Jian Zhang,*[ab] Ying Zhang,[a] Lutao Li,[b] Wei Yan,[a] Haiyun Wang,[a] Weiwei Mao,*[a] Yan Cui,*[c] Yonghua Li,[b] and Xinbao Zhu[d]

[a]New Energy Technology Engineering Lab of Jiangsu Province, College of Science, Nanjing University of Posts & Telecommunications (NUPT), Nanjing 210023, P. R. China.

[b]State Key Laboratory of Organic Electronics and Information Displays, Institute of Advanced Materials (IAM), Nanjing University of Posts and Telecommunications (NUPT), Nanjing 210023, Jiangsu, P. R. China

[c]Key Laboratory of Broadband Wireless Communication and Sensor Network Technology, Ministry of Education, Nanjing University of Posts and Telecommunications, Nanjing 210003, P. R. China

[d]College of Chemical Engineering, Nanjing Forestry University, Nanjing 210037, P. R. China.

E-mail: iamjzhang@njupt.edu.cn (Jian Zhang); maoww@njupt.edu.cn (Weiwei Mao); cuiyan@njupt.edu.cn (Yan Cui);

1.Experimental section

1.1. Samples preparation

All the chemicals were purchased from Sigma-Aldrich and used without further purification. $BiFeO_3$ is prepared by a simple hydrothermal method. Typically, 2.425 g (0.005 mol) bismuth nitrate pentahydrate and 2.020 g (0.005 mol) iron nitrate nine hydrate were dissolved in 22 mL nitric acid solution (1 M). After 0.5 h continuous stirring, the above colorless and transparent solution was added dropwise into 30 mL solution containing 8.5 g potassium hydroxide, and then centrifuged and washed with deionized water to obtain the precipitate. Then, the precipitation was dispersed into deionized water and 2.0 g PEG 10000 as well as potassium hydroxide were added. The solution volume is ~40 mL and the concentration of potassium hydroxide was 10 M. After stirring for 15 min, the mixed solution was transferred into a 50 mL Teflon-lined autoclave, followed by 130 °C for 36 h. After the reaction, the sample was washed with deionized water and ethanol three times, respectively.

For $BiFeO_3/ZnIn_2S_4$ core/shell heterojunction, 200 mg of the obtained $BiFeO_3$ powder was dispersed in 20 mL of deionized water and ultrasonicated for 30 min, and 5 mL of glycerin was added for another 30 min. Then a certain amount of zinc acetate dihydrate, anhydrous indium chloride and thioacetamide (the molar ratio is 1 : 2 : 4) were added and the obtained solution was stirred for 15 min. Next, the solution was stirred in an oil bath at 80 °C for 2 hours. After the reaction, the product was collected by centrifugation at 8000 rpm for 5 minutes, washed with deionized water and ethanol three times and dried at 60°C for 12 hours. The different amount of zinc acetate dihydrate for different nanohybrids were labeled as ZB-1, ZB-2, ZB-3 and ZB-4, respectively (0.001 mol for ZB-1, 0.002 mol for ZB-2, 0.003 mol for ZB-3 and 0.004 mol for ZB-4).

1.2. Characterization

The X-ray diffraction (XRD) was carried out on a D8 Advance X-ray powder diffractometer with Cu Ka radiation with a scan speed of 0.5 s per step. The morphologies of the samples were characterized by transmission electron microscopy (TEM) (FEI Tecnai F20) at an acceleration voltage of 200 kV. Scanning transmission electron microscopy (STEM) was performed using a FEI Titan 80-200 (ChemiSTEM) electron microscope operated at 200 kV, equipped with a high angle annular dark field (HAADF) detector, while compositional maps were obtained with energy dispersive spectroscopy (EDS) using four large solid-angle symmetrical Si drift detectors. The scanning electron microscopy (SEM) images were obtained on a scanning electron microscope (Hitachi S-4800). The X-ray photoelectron spectra images (XPS) were performed on a ESCALAB 250i X-ray photoelectron spectrometer monochromatic Al Kα radiation. PL spectra was tested by FLS920 spectrograph. TRPL was performed on Edinburgh FL/FSTCSPC920. ESR was conducted on JES-X320 spectrometer using DMPO (50 mm) solution as paramagnetic species spin-trap agent. The BET surface area was measured using the nitrogen gas adsorption-desorption method (TriStar II 3020) at 77 K. KPFM (Bruker) technique performs measurements of surface potential in the amplitude-modulated (AM) mode by exciting the cantilever electrically and mechanically at the same time under an ambient atmosphere. The contact potential difference (CPD) is defined as the surface work function difference between tip and sample. Transient absorption (TA) measurements were carried out in air using the third harmonic of a Nd:YAG laser (EKSPLA, NT 342B, 410 nm, 5 ns pulse width, 0.9 Hz) as the pump source. An optical fiber transmitted the laser pulse to the sample resulting in an incident pump intensity of ca. 300 μJ cm^{-2} (410 nm). A 100 W tungsten lamp (Bentham, IL 1) coupled to a monochromator (Zolix, Omni - λ 300) was used as the probe light. Variation in optical density (ΔOD) of the sample was calculated by measuring the transmitted light using a Si photodiode (Hamamatsu) and an amplification system coupled to both an oscilloscope (Tektronix, TDS 2012C) and data acquisition card (National Instruments NI-6221). The data were averaged over 400 laser shots. The SPV was directly related to the photogenerated charge separation, whose amplitude and sign denoted the ability of the charge separation and the direction of charge transport, respectively. Inductively coupled plasma atomic emission spectrometry (ICP-AES) analysis was performed on a Thermo ICAP-6300 instrument (USA). The femtosecond time-resolved transient absorption (fs-TA) spectroscopy were carried out in air using the third harmonic of a Nd:YAG laser (EKSPLA, NT 342B, 410 nm, 5 ns pulse width, 0.9 Hz) as the pump source. An optical fiber transmitted the laser pulse to the sample resulting in an incident pump intensity of 300 μJ cm^{-2} (410 nm). A 100 W tungsten lamp (Bentham, IL 1) coupled to a monochromator (Zolix, Omni -λ 300) was used as the probe light. Variation in optical density (ΔOD) of the sample was calculated by measuring the transmitted light using a Si photodiode (Hamamatsu) and an amplification system coupled to both an oscilloscope (Tektronix, TDS 2012C) and data acquisition card (National Instruments NI-6221). The data were averaged over 400 laser shots.

1.3. Photocatalytic hydrogen and oxygen production half-reactions measurements

Photocatalytic measurements were carried out at a constant temperature (20 °C) in a closed gas circulation system. In photocatalytic hydrogen evolution half-reaction, the obtained photocatalyst powder (20 mg) was dispersed in 150 mL of aqueous solution containing 0.25 M Na_2SO_3 and 0.35 M Na_2S as the photogenerated holes sacrificial reagents. A 300 W Xe lamp (91160, Newport, USA) equipped with a UV-light cut-off filter ($\lambda > 420$ nm) was used to provide visible light. The evolved gases were analyzed on-line using a gas chromatography equipped with a thermal conductivity detector (TCD) and a molecular sieve 5Å column. Photocatalytic oxygen evolution halfreactions were carried out under the same conditions except that 20 mM $NaIO_3$ aqueous solution was adopted as the photogenerated electrons sacrificial reagent.

1.4. Photocatalytic overall water splitting reaction

Photocatalytic overall water splitting reactions were carried out under the conditions similar to the photocatalytic hydrogen evolution and oxygen evolution half-reactions as described above ($\lambda > 420$ nm), except that the photocatalyst powder (12 mg) was dispersed in 100 mL of distilled water without the presence any sacrificial reagents. The AQE of the photocatalytic reaction was calculated using the following equation:

$$\mathrm{AQE}[\%] = \frac{\text{number of reacted electrons}}{\text{number of incident photons}} \times 100$$
$$= \frac{\text{number of evolved } H_2 \text{ molecules} \times 2}{\text{number of incident photons}} \times 100\ \%$$

For AQE measurements, several band-pass filters with full width at half maximum (FWHM) of 15 nm were employed to achieve the desired incident light wavelength under a 300 W xenon lamp (91160, Newport, USA). The outputting light density of each irradiation wavelength was determined by an optical power meter (PM100D, Thermal Powermeter Head, THORLABS).

1.5. Photoelectrochemical (PEC) measurements

Fabrication of PEC Sensor: prior to modification, the ITO glass (1 cm × 2 cm) was cleaned by successive sonication in NaOH solution (1 M), acetone, ethanol, and pure water, each for 20 min. After being dried at 60 °C in an oven, a 3M tape with a fixed area of 0.080 cm^2 was stuck on the ITO glass. Then, 15 μL (1 mg mL^{-1}) of aqueous dispersion of sample was dropped onto the ITO surface and dried at 60 °C to obtain the $ZnIn_2S_4/BiFeO_3$/ITO working electrode. PEC properties were measured on a standard three-electrode potentiostat system (CHI660D, Chenhua, Shanghai) with a working electrode, a Pt counter electrode, and a Hg/Hg_2Cl_2 reference electrode. The amperometric current-time curves were recorded using 300 W Xenon lamp (91160, Newport, USA) equipped with an optical filter ($\lambda > 420$ nm) under light on/off cycles. The EIS Nyquist plots were collected under the open-circuit condition with the frequency ranging from 0.1 Hz to 100 kHz and the modulation amplitude of 5 mV.

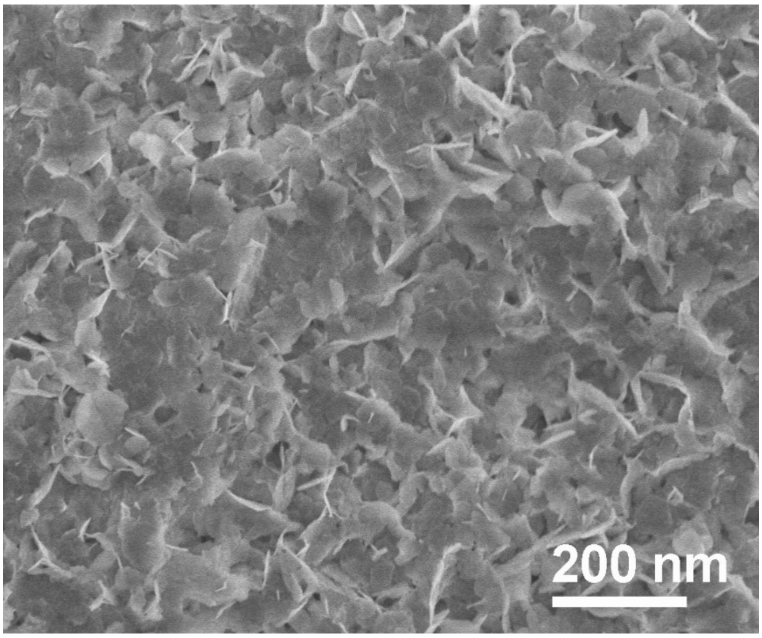

Fig. S1 SEM image of $ZnIn_2S_4$.

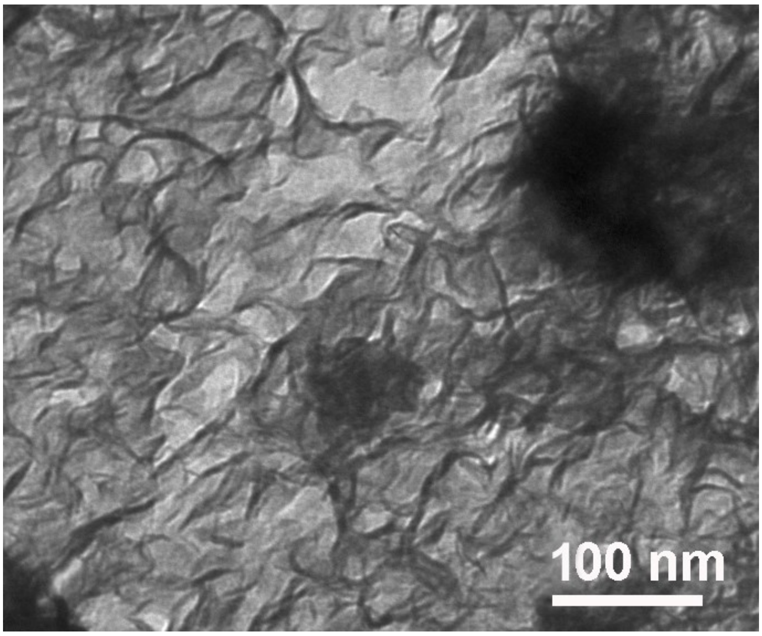

Fig. S2 TEM image of $ZnIn_2S_4$.

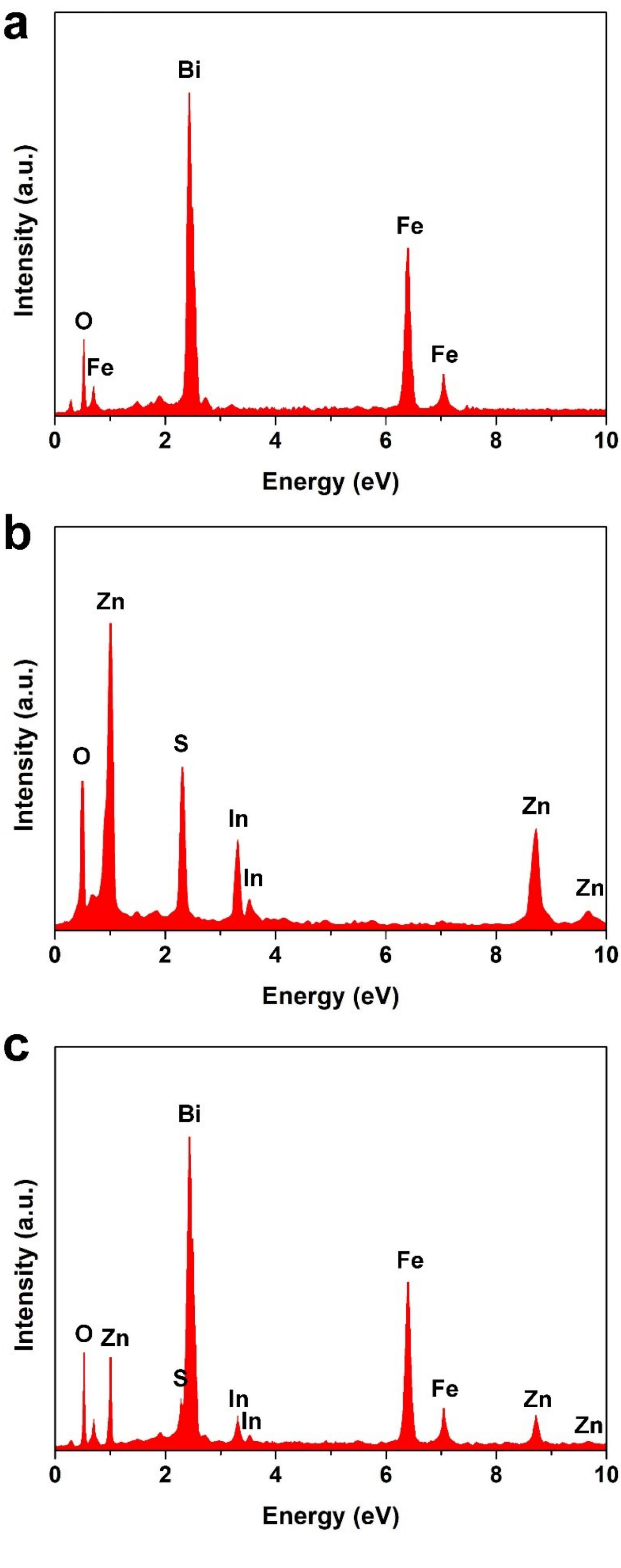

Fig. S3 EDS spectrum of (a) $BiFeO_3$, (b) $ZnIn_2S_4$ and (c) ZB-3.

Table S1 ICP-AES of the as-obtained photocatalysts.

Sample		Bi content / μg 209	Fe content / μg 55.9	Zn content / μg 65.4	In content / μg 114.8	In mass percentage / %
$BiFeO_3$	1463.2		391.1	—	—	—
$ZnIn_2S_4$	—		—	359.7	1262.8	—
ZB-1	Before	1421.6	380.1	11.6	40.7	2.2
	After	1472.2	385.6	9.3	36.9	2.0
ZB-2	Before	1295.8	346.6	28.7	100.7	5.4
	After	1331.0	368.8	26.7	95.5	5.1
ZB-3	Before	1149.5	279.5	42.7	149.9	8.1
	After	1155.3	295.7	41.7	146.6	8.0
ZB-4	Before	1003.2	268.3	75.5	265.0	14.3
	After	1054.1	291.2	71.7	259.7	11.9

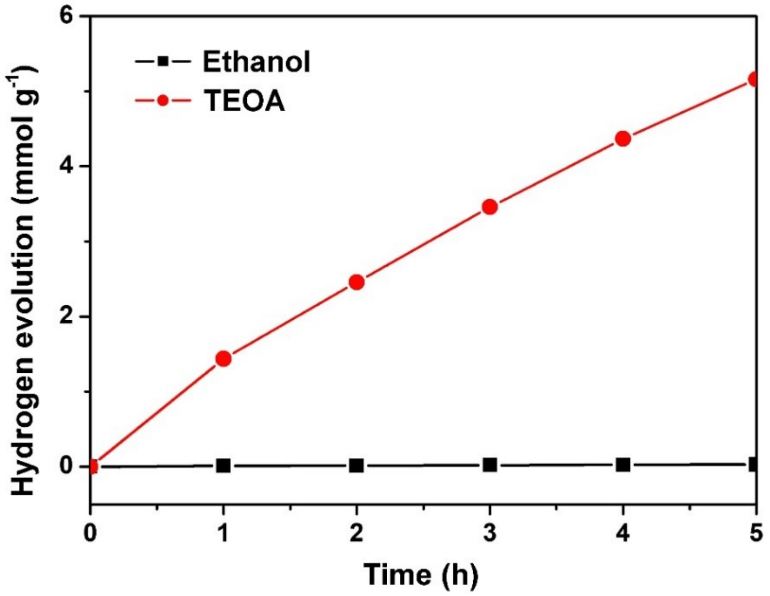

Fig. S4 Photocatalytic hydrogen production rate of ZB-3 under ethanol and TEOA sacrificial agents.

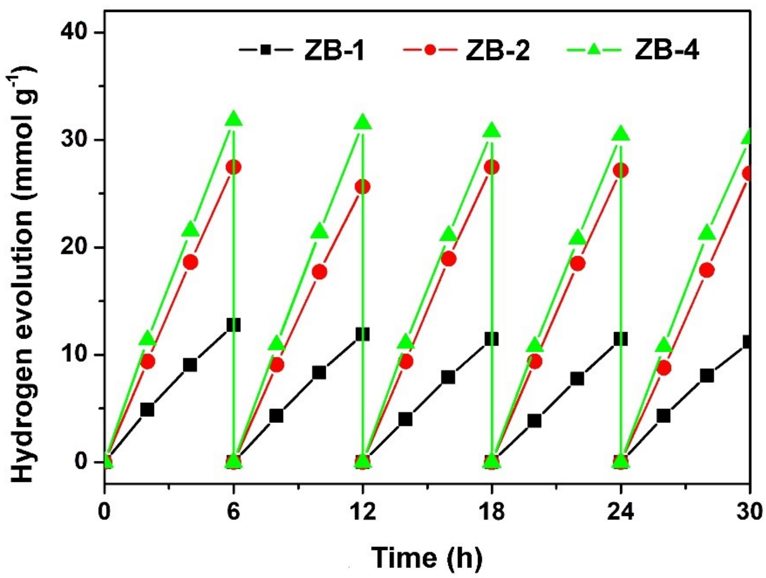

Fig. S5 Photocatalytic HER cycles over ZB-1, ZB-2 and ZB-3.

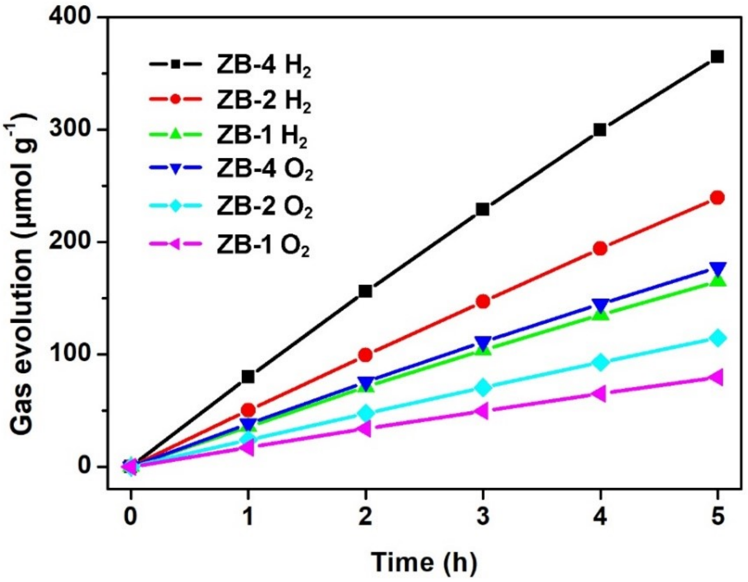

Fig. S6 Time-dependent of photocatalytic overall water splitting over ZB-1, ZB-2, ZB-3and ZB-4.

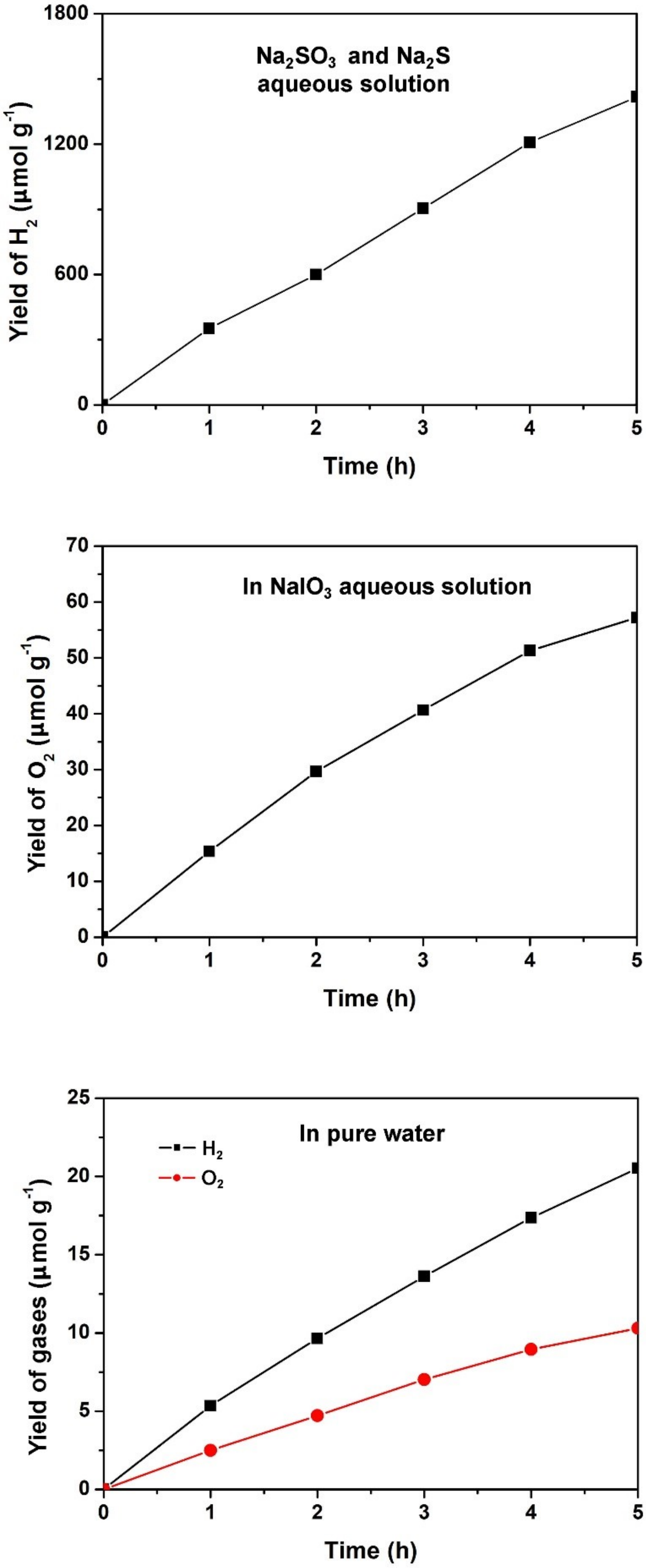

Fig. S7 The photocatalytic hydrogen evolution half-reaction, oxygen evolution half-reaction and overall water splitting of the physic mixture sample.

Table S2 Summary of heterojunction-based materials for photocatalytic overall water splitting activity.

Catalysts	Co-catalyst	Light Source	H_2 (μmol h^{-1})	O_2 (μmol h^{-1})	AQE (420 nm)	Ref.
$BiFeO_3$/ $ZnIn_2S_4$	**--**	**λ > 420 nm**	**87.32**	**42.33**	**1.12 %**	**This work**
$BiVO_4$/ Ti_3C_2	--	AM-1.5	2.25	1.11	1.47 %	1
$SrTiO_3$ /TiO_2	--	λ ≥ 365	10.6	5.12	2.6 %	2
g-C_3N_4/ rGO/PDIP	Pt, $Co(OH)_2$	λ ≥ 420 nm	15.8	7.8	4.94 %	3
CdS/Ni_2P/CN	--	λ ≥420 nm	0.78	0.39	0.18 %	4
$PtMO_x$/ CN-M	Co_3O_4	λ ≥420 nm	2.38	1.14	0.10 %	5
MnO_2/ g-C_3N_4	--	λ ≥420 nm	60.6	28.9	--	6
g-C_3N_4/ $BiFeO_3$	--	λ ≥400 nm	16.25	5.10	--	7
C_3N_4/rGO /Fe_2O_3	WO_3	λ ≥400 nm	43.6	21.2	--	8
$ZnIn_2S_4$/WO_3	PtS/MnO_2	λ ≥420 nm	0.71	0.28	0.50 %	9
$NiCo_2O_4$/ C_3N_4	Pt	λ ≥400 nm	22.6	11.0	0.92 %	10

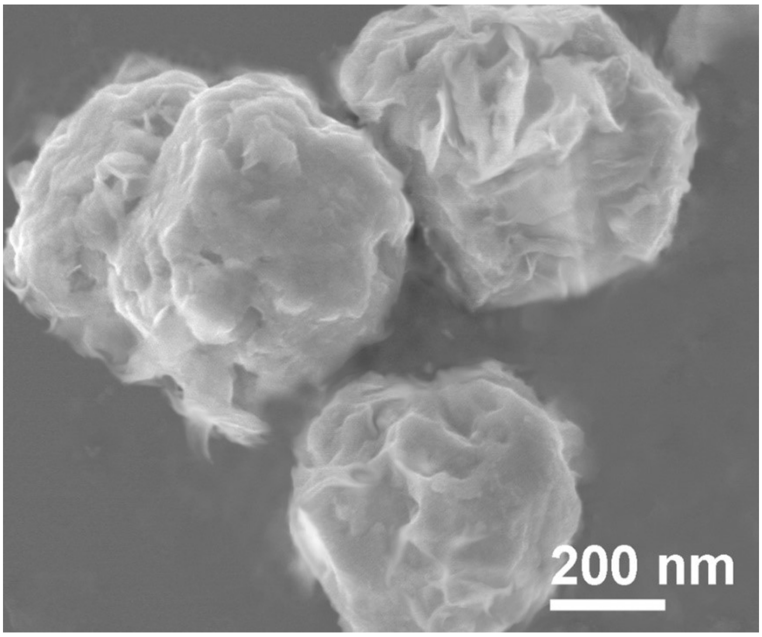

Fig. S8 SEM image of ZB-3 after cycle tests.

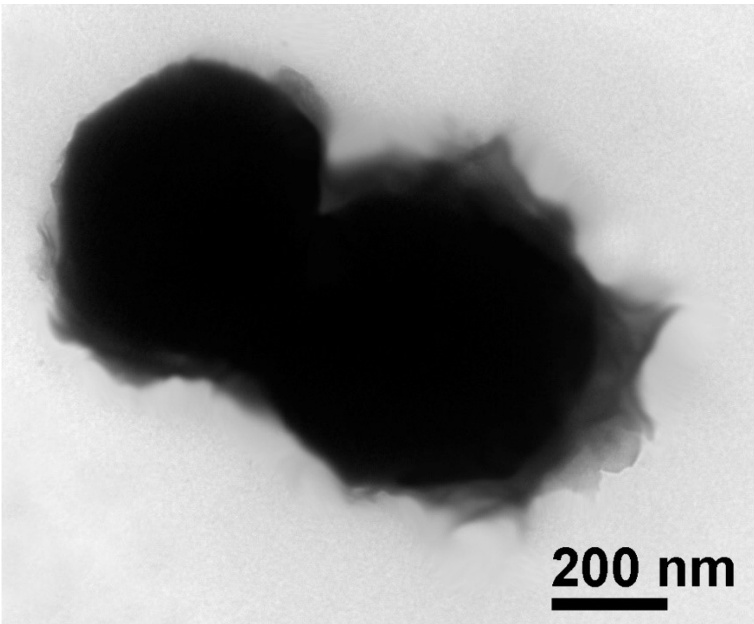

Fig. S9 TEM image of ZB-3 after cycle tests.

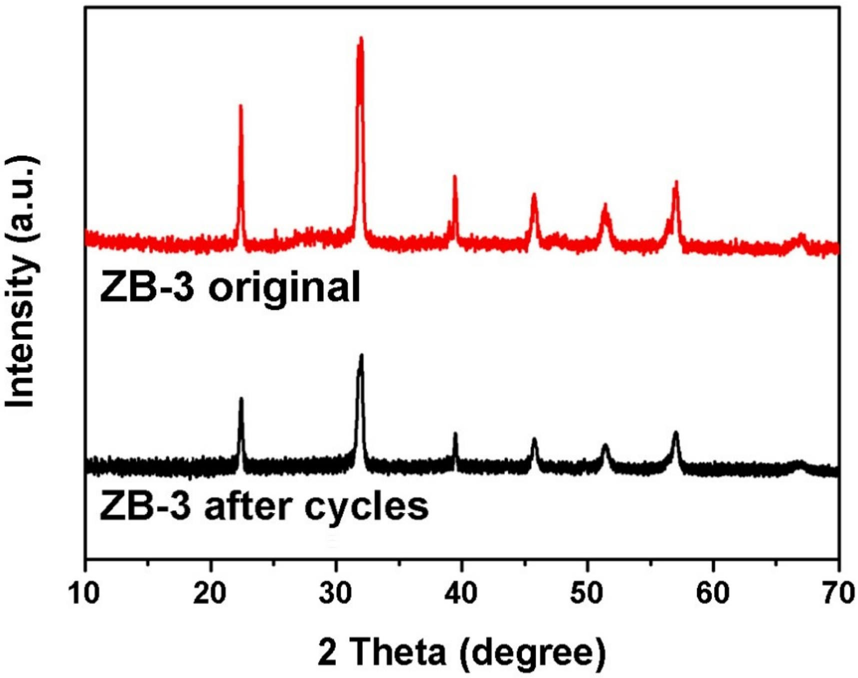

Fig. S10 XRD patterns of ZB-3 before and after cycle tests.

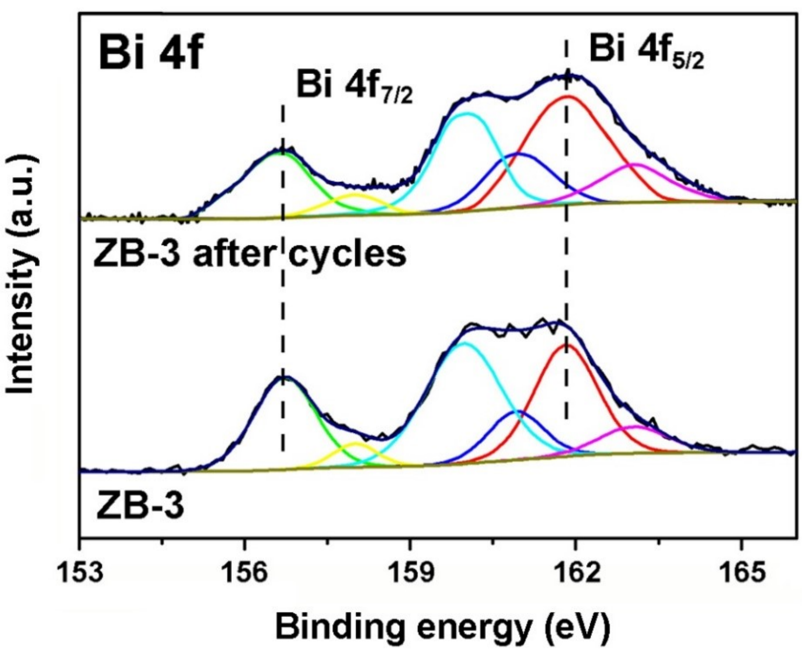

Fig. S11 Bi 4f XPS spectra of ZB-3 before and after cycle tests.

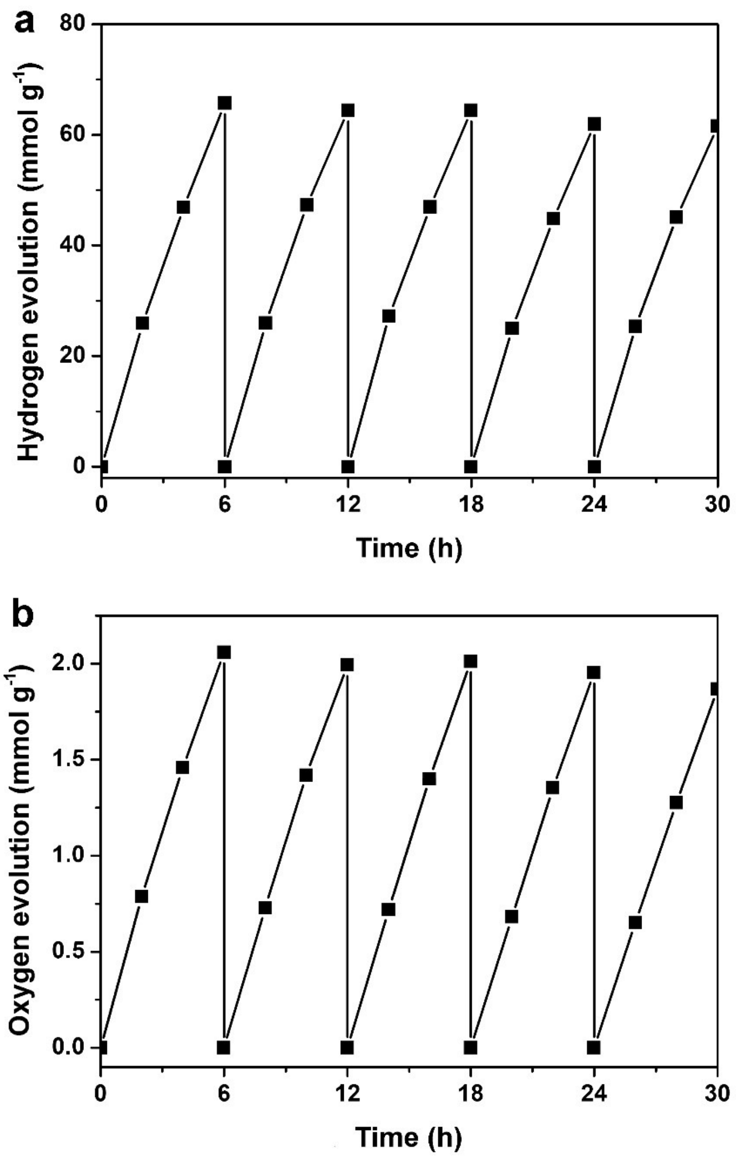

Fig. S12 The recycling performance of ZB-3 towards photocatalytic half-reaction.

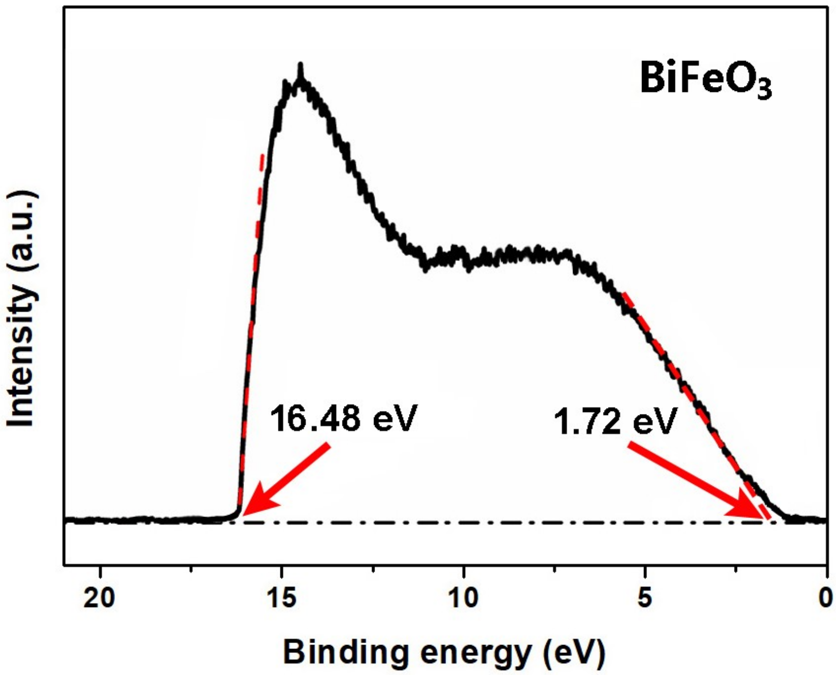

Fig. S13 UPS spectra of the $BiFeO_3$.

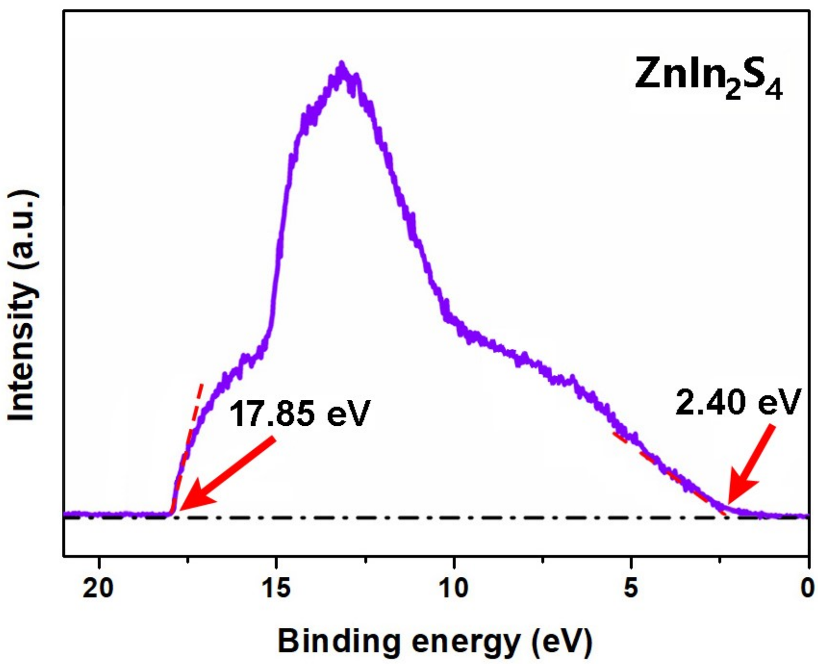

Fig. S14 UPS spectra of the $ZnIn_2S_4$.

References

[1] Y. Li, Y. Liu, D. Xing, J. Wang, L. Zheng, Z. Wang, P. Wang, Z. Zheng, H. Cheng, Y. Dai, B. Huang, Appl. Catal. B: Environ., 2021, 285, 119855.

[2] Y. Wei, J. Wang, R. Yu, J. Wan, D. Wang, Angew. Chem., Int. Ed., 2020, 59, 1422-1426.

[3] X. Chen, J. Wang, Y. Chai, Z. Zhang, Y. Zhu, Adv. Mater., 2021, 33, 2007479.

[4] H. He, J. Cao, M. Guo, H. Lin, J. Zhang, Y. Chen, S. Chen, Appl. Catal. B-Environ., 2019, 249, 246.

[5] Z. Zeng, X. Quan, H. Yu, S. Chen, W. Choi, B. Kim, S. Zhang, J. Catal., 2019, 377, 72.

[6] Z. Mo, H. Xu, Z. Chen, X. She, Y. Song, J. Lian, X. Zhu, P. Yan, Y. Lei, S. Yuan, H. Li, Appl. Catal. B-Environ., 2018, 241, 452-460.

[7] H. Sepahvand, S. Sharifnia, In. J. Hydrogen Energy, 2019, 44, 23658-23668.

[8] Z. Pan, G. Zhang, X. Wang, Angew. Chem. Int. Ed., 2019, 58, 7102-7106.

[9] Y. Ding, D. Wei, R. He, R. Yuan, T. Xie, Z. Li, Appl. Catal. B-Environ., 2019, 258, 117948.

[10] C. Cheng, L. Mao, J. Shi, F. Xue, S. Zong, B. Zheng, L.Guo, J. Mater. Chem. A, 2021, 9, 12299-12306.